Oil Shale, 2020, Vol. 37, No. 2, pp. 89–103
doi: https://doi.org/10.3176/oil.2020.2.01
ISSN 0208-189X

Analysis of the pore structure of Longkou oil shale semicoke during fluidized bed combustion

Hongpeng Liu[(a)*], Shiyu Feng[(a)], Shiqiang Zhang[(a)], Haoran Xuan[(b)], Chunxia Jia[(a)], Qing Wang[(a)]

[(a)] Engineering Research Centre of Oil Shale Comprehensive Utilization, Ministry of Education, School of Energy and Power Engineering, Northeast Electric Power University, Jilin 132012, China
[(b)] Shandong Electric Power Engineering Consulting Institute Corp, Ltd, Jinan 250013, China

Abstract. *The combustion experiment of Longkou oil shale semicoke was conducted in a batch fluidized bed reactor. A specific surface area (SSA) analyzer and a scanning electron microscope (SEM) were used to respectively measure the specific surface area of samples and examine their surface pore structure in different experimental operating conditions, and the fractal dimension (FD) was used to describe the complexity of pore morphology. The results showed that Longkou oil shale semicoke had a developed pore structure, and in the combustion process, its SSA and pore volume first increased and then decreased, remaining finally unchanging. Most pores were micropores and mesopores of about 2 nm in size. The pore structure was fully developed at a temperature of 600 °C, at which the specific surface area and pore volume also reached maximum values. There were great differences in the pore size distribution of semicoke with different particle sizes. As calculated by the box-counting method (BCM) and the Frenkel-Halsey-Hill (FHH) equation, the pore size showed similar trends of variation, increasing first and then decreasing slowly.*

Keywords: *oil shale semicoke, fluidized bed combustion, nitrogen adsorption, pore structure analysis, fractal dimension.*

1. Introduction

Oil shale is a kind of sedimentary rock with high ash and low fixed carbon [1]. As an important supplementary resource to replace conventional fossil energy, oil shale has large reserves and is relatively concentratedly distributed. At present, oil shale is mainly used to produce shale oil by retorting and generate power by combustion in the industrial development and utilization [2]. The industrial applications of oil shale also include oil production by

* Corresponding author: e-mail *hongpeng5460@126.com*

pyrolysis and energy production by combustion using pulverized firing and circulating fluidized bed [3]. Researchers have conducted many studies on oil shale, such as the characterization of pyrolysis waste water from oil shale industry, simulation of oil shale combustion in a circulating fluidized bed, and environmental protection measures to be taken during oil shale exploitation [4, 5].

A large amount of solid waste, oil shale semicoke, is produced in the process of shale oil production by retorting. Oil shale semicoke has a secondary utilization value. Researchers at home and abroad believe that semicoke can be utilized in fluidized bed combustion, and this has already been done in Enefit280 technology [6, 7]. High-calorific semicoke can be directly burned, while low-calorific semicoke can be co-combusted with either high-calorific oil shale, coal or biomass, which not only utilizes semicoke, but also reduces its environmental hazards [8]. Trikkel et al. [9] carried out a circulating fluidized bed combustion experiment on Estonian oil shale semicoke and found that low-moisture semicoke can be burned directly in a fluidized bed. For higher-moisture semicoke (over 10%), about 10% of oil shale must be added to enable co-combustion to take place. Kaljuvee et al. [10] conducted a series of experiments on oil shale semicoke in a laboratory fluidized bed. It was concluded that using the circulating fluidized bed technology for utilization of semicoke, SO_2 could be fully assimilated by the solid phase. Zanoni et al. [11] established and optimized the chemical combustion mechanism of oil shale and its semicoke and determined kinetic parameters which affected the drying, pyrolysis, oxidation and decarbonation reactions. Liu et al. [12] analyzed the combustion of a mixture of oil shale semicoke and cornstalk particles under different conditions in a circulating fluidized bed. The researchers found that with increasing cornstalk portion in the mixture, the combustion characteristics of semicoke were improved, the furnace exit temperature was elevated, the concentrations of O_2 and CO were decreased and the content of combustibles in the bottom ash gradually fell below 2%. Sun et al. [13] studied the thermal fragmentation of Huadian oil shale semicoke in fluidized bed combustion. The fragmentation was observed to take place mainly on the surface of the semicoke particles. The fragmentation index increased with increasing particle size, bed temperature, residence time and fluidization velocity.

The chemical reactions of fossil fuel such as combustion, pyrolysis and gasification mostly take place in the pores of its particles. During these reactions the fuel particles pore structure undergoes great changes, which in turn affects the progress of the combustion reaction as a whole, revealing at the same time its mechanism. By the present time, several scholars have studied the pore structure of oil shale semicoke. Külaots et al. [14] studied the characteristics of semicoke of eight oil shales from China, Estonia and the United States. The researchers found that semicoke was mostly pyrolyzed at 1000 °C, while mesopores developed into micropores in the surface area of semicoke particles. Huang et al. [15] examined the pore structure of

Huadian oil shale semicoke prepared at different retorting temperatures and with different residence times. The results showed that the specific surface area (SSA) and specific volume of oil shale semicoke first increased and then decreased with the increase of retorting temperature. The SSA of oil shale semicoke first increased and then decreased with increasing residence time, while the specific pore volume increased steadily. Zhao et al. [16] researched the pore structure of oil shale and its semicoke at different final temperatures, and found that the pores in oil shale were open in one direction, while those in semicoke were open in two to even four directions. Bai et al. [17] investigated the effect of heating rate on the pore structure of Huadian oil shale semicoke. The SSA and total pore volume of semicoke were shown to decrease with the increase of heating rate. Qin et al. [18] found that the pore structure of oil shale semicoke had already been well developed, and its total pore volume gradually decreased during combustion, while the low combustion temperature was favorable for the further development of the pore structure

To date, there have been several reports on the surface pore structure changes of coal and coal char particles during combustion and pyrolysis [19, 20]. However, there are only a few studies on the combustion mechanism and surface pore structure changes of oil shale. In this paper, Longkou oil shale semicoke is used as experimental material and is burned in a batch fluidized bed reactor. The SSA and pore structure of ash particles under different combustion conditions are analyzed using an SSA analyzer, and changes of oil shale semicoke surface pore structure during fluidized bed combustion are studied in depth.

2. Experimental materials and methods

2.1. Experimental sample

The experimental raw oil shale is from Longkou, China, and the process of preparing semicoke was described in ASTM D3904-90 Test Method for Oil From Oil Shale (Resource Evaluation by the Fischer Assay Procedure), according to which, raw oil shale was dried, crushed and then stored in a desiccator. The oil shale sample was put into an aluminum retort to produce 500 °C semicoke, screen out the required particle size and store in a sealed bottle. The basic characteristics of oil shale semicoke are given in Table 1.

Table 1. Basic characteristics of Longkou oil shale semicoke

Proximate analysis, %, ad				Ultimate analysis, %, ad					Low calorific value, kJ kg^{-1}	BET area, m^2 g^{-1}	Pore volume, cm^3 g^{-1}
M	V	A	FC	C	H	O	N	S	$Q_{net,ar}$	S	V
3.80	17.62	65.75	12.83	21.36	1.74	0.50	6.13	0.72	6888.79	12.1148	0.0502

Note: ad – air-dried basis; M – moisture, V – volatile matter; A – ash; FC – fixed carbon; ar – as received.

Figure 1 shows the schematic of the batch fluidized bed reactor [21] used in this study. The air speed was 0.72 m/s, each feed was 3 g, and quartz sand with a particle size ranging from 0.335 to 0.5 mm was used as bed material. When the temperature reached the specified temperature, the semicoke sample was added into the reactor. When the burning time reached the preset value, air was replaced by nitrogen to terminate the combustion. After the system was cooled, the bed material was removed and the sample was separated from the bed material. The experimental conditions of fluidized bed combustion are presented in Table 2.

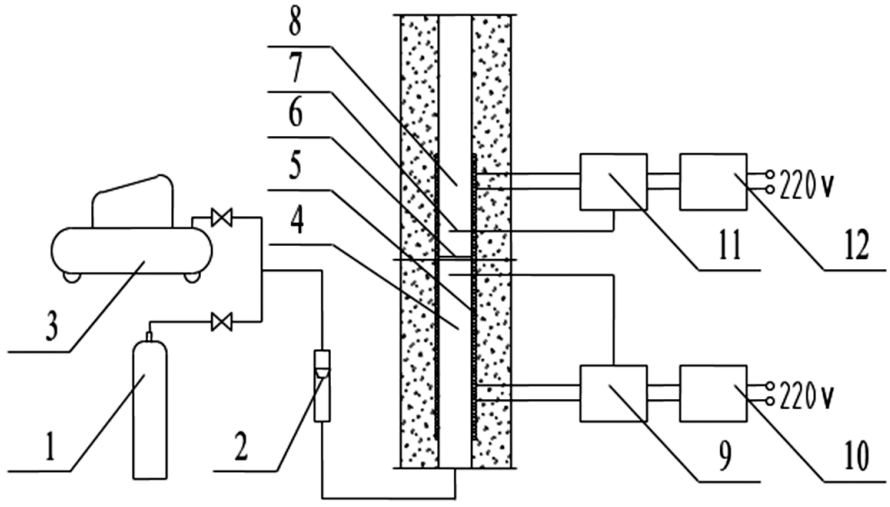

Fig. 1. Schematic of the batch fluidized bed reactor: 1 – high-purity nitrogen; 2 – rotameter; 3 – compressed air; 4 – preheating section; 5 – thermocouple 1; 6 – distribution plate; 7 – thermocouple 2; 8 – reaction section; 9 – temperature controller 1; 10 – voltage regulator 1; 11 – temperature controller 2; 12 – voltage regulator 2.

Table 2. Experimental conditions of fluidized bed combustion

Combustion time, s	Bed temperature, °C	Semicoke particle size, mm
0, 10, 20, 40, 60, 180	400, 500, 600, 700, 800, 850, 900	1–4, 1–2, 3–4

2.2. Low-temperature nitrogen adsorption isotherm method

The specific surface area and pore structure parameters of samples were determined on a TriStar II 3020 automatic specific surface area and porosity analyzer. The instrument consists of three parts: analysis station, degassing station and computer. The samples were degassed at 200 °C under a pressure of 0.334 MPa for 4 hours in nitrogen atmosphere to clean the surface of particles. Nitrogen (99.999%) was physically adsorbed into a degassed sample at the temperature of liquid nitrogen (77 K) in the relative pressure P/P_0 range of 0.01–0.995 where P and P_0 represent balance pressure and saturation pressure, respectively. The pore diameter range was 0.35–500 nm, and the isothermal adsorption and desorption experiments were carried out to obtain the adsorption-desorption isothermal curve, to have information on oil shale semicoke pore structure. The SSA was obtained by linear regression according to the Brunauer-Emmett-Teller (BET) equation, and the pore distribution was calculated by the Barrett-Joyner-Halenda (BJH) model. Similarly, scanning electron microscopy (SEM) experiments of different semicoke samples were performed. The JSM-7610F scanning electron microscope was used to obtain SEM images of the samples.

3. Results and discussion

3.1. Effect of reaction time on pore structure

Figure 2 shows the variation of the specific surface area and pore volume of total and micropores of the sample, respectively, during combustion at 850 °C. The original semicoke sample had a relatively large specific surface area. The SSA of the sample increased to a peak value within 0–10 s, thereafter rapidly decreased during the next 10–60 s, and finally became moderate after 60–180 s. Such a variation of SSA was mainly due to the high content of volatile matter and the low content of fixed carbon of oil shale semicoke. In the initial stage, the combustion reaction of the sample was more intense and its SSA increased noticeably. However, with increasing reaction time, new pores formed during combustion were merged, which resulted in a decrease in SSA. In a later stage of combustion, semicoke had almost completely reacted, and its SSA and pore volume no longer changed. The trend of change of the pore volume of micropores was similar to that of the SSA of the samples. The microporous specific surface area and pore volume of the semicoke sample were relatively small because the volatile matter produced by semicoke pyrolysis was in a semi-precipitated state and partly blocked the formation of micropores. In the initial stage of combustion, semicoke released a large amount of volatiles, resulting in the formation of numerous micropores on the ash surface, so their SSA and pore volume increased sharply. Combining the surface area and pore volume change curves of total pores, it was found that in the initial stage of combustion, the SSA increased and pore volume decreased, indicating that the

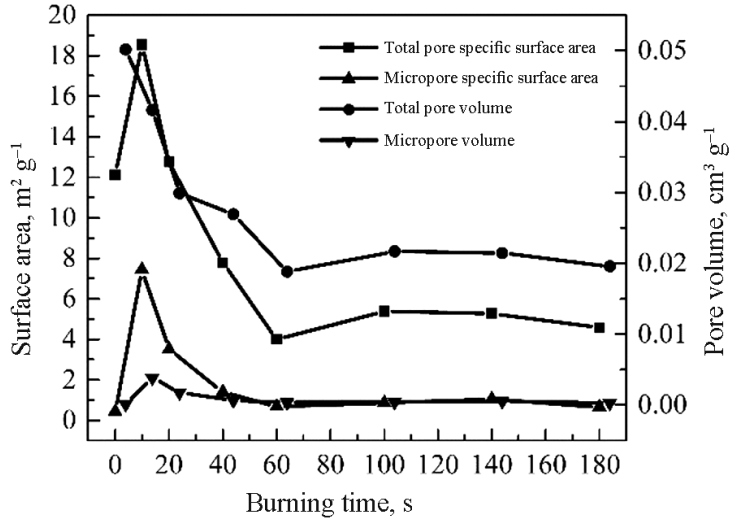

Fig. 2. Variation of the specific surface area and pore volume of total and micropores of semicoke (per gram) during combustion.

formation of micropores on the semicoke surface took place rapidly while that of mesopores and macropores continuously failed. Similarly, with increasing reaction time, the SSA and pore volume of micropores gradually decreased to become constant eventually.

Figure 3a depicts an adsorption-desorption isotherm of Longkou oil shale semicoke. Although the shape of the adsorption isotherm of the sample slightly varied during combustion, as a whole, it was inverse S-shaped. According to the BET classification, the curve belonged to type II adsorption isotherms [17]. The micropore filling phenomenon occurred in the low pressure section, and the curve was slightly convex upward, which indicated that the interaction force between the sample and the adsorbate was strong, and monolayer adsorption became multi-molecular layer adsorption. With the pressure increasing, the adsorption amount in the medium pressure section increased slowly, and the small pores were gradually filled with the coacervate, which represented the multi-molecular layer adsorption process. The capillary condensation occurred in the high pressure section, the adsorption line ascended vertically, and no adsorption saturation occurred at a place where the relative pressure was close to 1.0. When the relative pressure was about 0.8, the adsorption and desorption isotherms were separated and a hysteresis loop was formed. According to the International Union of Pure and Applied Chemistry (IUPAC) classification [22], the sample desorption loop belonged to H3 type, indicating that the sample had an irregular porous structure (fractured and wedge-shaped pores), which may be related to the thin layer structure of clay mineral in semicoke. It was further found that the residence time had a great influence

on the adsorption capacity of the sample, but its adsorption at 60 s and 180 s was approximately the same, indicating that semicoke had fully burned at 60 s. It can be seen from Figure 3b that the semicoke pore size was around 2 nm, implying that pores were mainly micro- and mesopores. As the reaction time increased, the total pore volume of the sample increased first and then decreased. This was mainly because of the secondary combustion of residual volatile matter and fixed carbon in semicoke during the initial stage of fluidized combustion, which resulted in the further development of the pore structure. In a later stage of combustion, a continuous collision and friction of semicoke with the furnace inner wall and bed material took place, the sample pore structure collapsed and underwent no further development, while organic matter had little effect on it, resulting in a continuous decrease in the total pore volume of the sample.

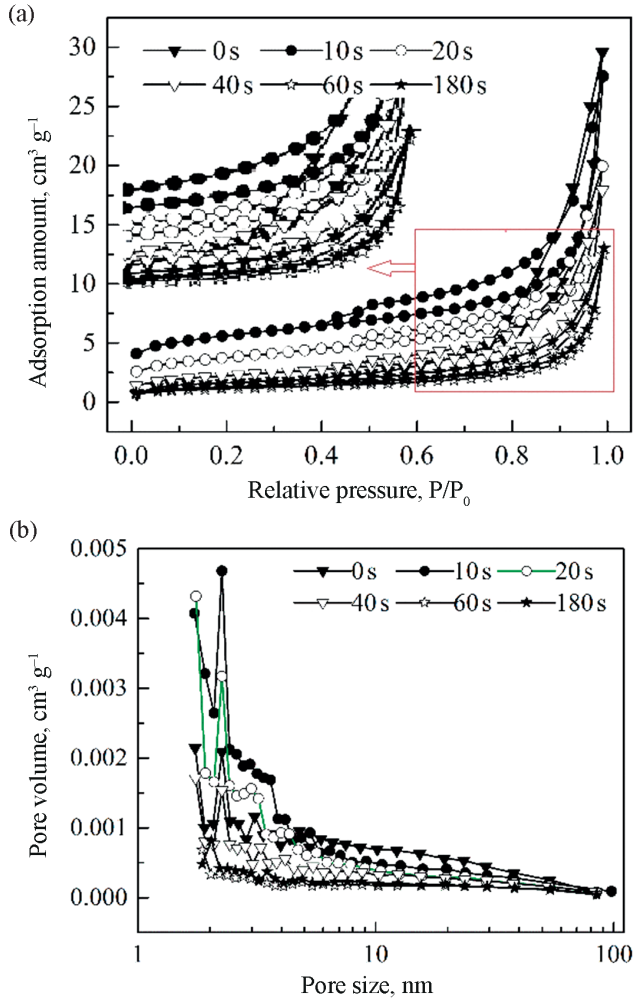

Fig. 3. The adsorption isotherm (a) and pore size distribution (b) for semicoke (per gram) with different residence times.

3.2. Influence of combustion temperature on pore structure

The semicoke sample with a particle size range of 1–4 mm was burned at 400 °C, 500 °C, 600 °C, 700 °C, 800 °C and 900 °C, respectively. It can be seen from Figure 4 that with increasing temperature the specific surface area and pore volume of Longkou oil shale semicoke first increase and then decrease. At the same time, Figure 2 shows that the SSA and pore volume of Longkou semicoke at 400 °C were close to those of the original sample. This was mainly because at a low combustion temperature the volatilization of volatile matter was incomplete, in semicoke it precipitated, the formation of pores was blocked, and the organic matter consumption was low, so, the pore structure was not fully developed and was greatly damaged. As the combustion temperature reached 500 °C, the volatile matter in semicoke was fully released, and the SSA and pore volume of the sample were significantly increased. When the temperature rose to 600–700 °C, the SSA and pore volume of the sample reached the maximum, and a more developed pore structure was formed. This was because the volatile matter volatilization was fully complete in this temperature range, and the pore structure collapse caused by the fixed carbon consumption and combustion damage was relatively small. When the temperature was over 700 °C, the SSA and pore volume of the sample decreased obviously. This suggested that the higher the temperature, the more intense the combustion, and, the higher the thermal stress, the more severe the fracture and collapse of the pore structure.

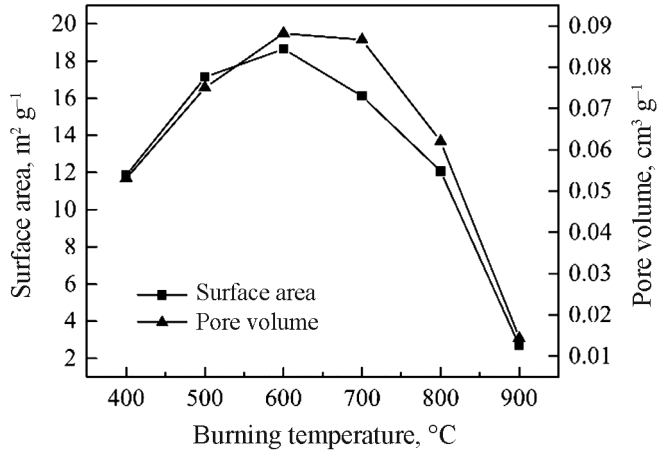

Fig. 4. Variation of the specific surface area and pore volume of semicoke (per gram) at different burning temperatures.

Figure 5 shows the adsorption isotherm and pore size distribution of Longkou oil shale semicoke (particle size 1–4 mm) at different burning temperatures during 180 s. The adsorption isotherm of the sample is of type II, and the desorption loop is close to type H3. Despite the different combustion temperatures, there were mostly micro- and mesopores within 10 nm in the structure of all semicoke samples. The combustion temperatures of 500 °C, 600 °C and 700 °C had the greatest influence on the semicoke pore size distribution. In the same temperature range, from 500 to 700 °C, semicoke and oil, which blocked the formation of micropores, were fully burned and the volatile matter was precipitated. It was also in this temperature region that, due to the consumption of organic matter, each pore below 10 nm in size was fully developed under pressure, so that the pore structure was the most developed and the adsorption amount was the largest, being in the high pressure section much higher than at 900 °C.

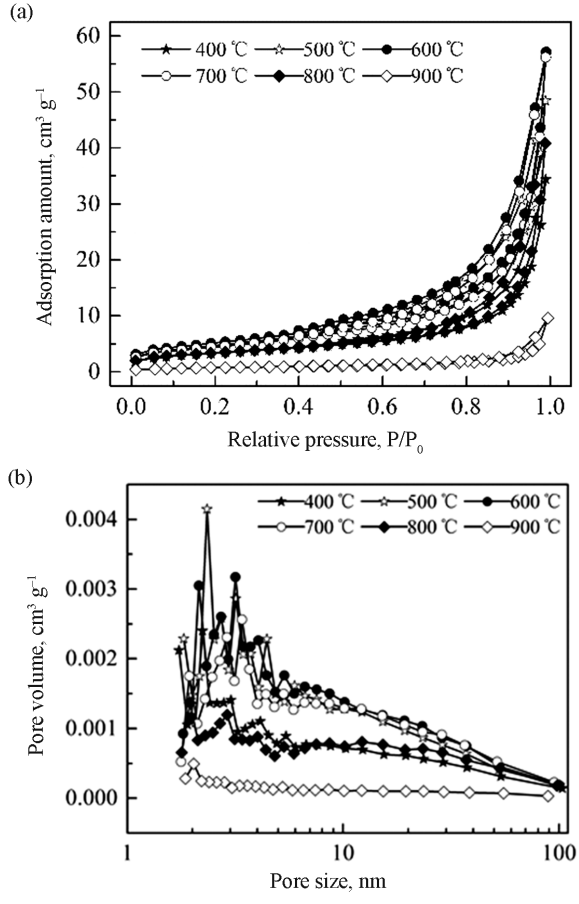

Fig. 5. The adsorption isotherm (a) and pore size distribution (b) of semicoke (per gram) at different burning temperatures.

3.3. Differences in pore structure of different-sized semicoke particles

The pore size distribution of Longkou oil shale semicoke with different particle sizes was different in the combustion process. The smaller the particle size of semicoke, the more complete the combustion, the larger the specific surface area involved in the reaction and the easier the precipitation of volatile matter. However, if the particles were too small, they were easily blown out of the furnace or fluidized above the furnace. As a result, there was not enough heat and the combustion was uneven. Therefore, samples with a particle size of 1–2 mm and 3–4 mm were used as research objects. As shown in Figure 6, on the pore size distribution line, the peak values of 3–4 mm particles are higher than those of 1–2 mm particles at a residence time of 10 s or 60 s. This might be due to that the heating of 3–4 mm semicoke particles was not even unlike 1–2 mm semicoke particles, and, as a result of slow combustion, most of the organic matter was retained in semicoke to contribute to the pore structure development. In the structure of semicoke with different particle sizes mainly 2 nm pores dominated, and the peaks of other pores tended to be flat.

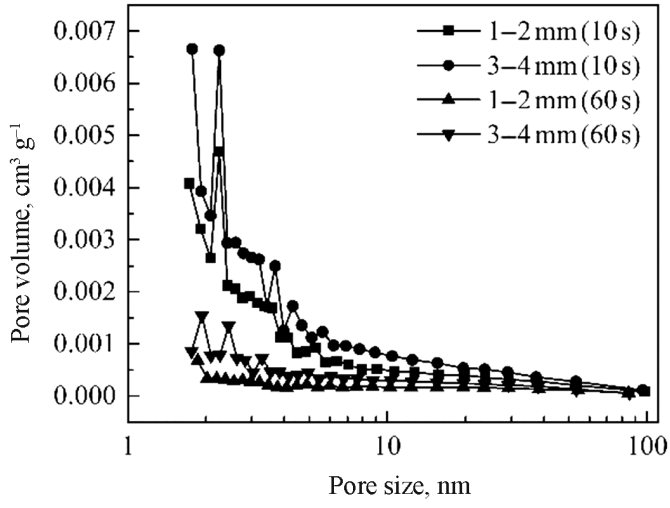

Fig. 6. Pore size distribution of semicoke (per gram) of different particle sizes at different residence times.

3.4. Micromorphology analysis of semicoke at different residence times

Figure 7 shows the micromorphology of the Longkou oil shale semicoke pore structure enlarged 5000 times at different residence times. It was found that the pore structure of Longkou semicoke was very complex, mainly with semi-closed wedge-shaped pores. At the beginning of combustion, there were gradually formed dense micropores on the semicoke sample surface, which was mainly caused by the organic matter released due to the secondary

combustion of residual volatile matter and fixed carbon. As the residence time increased, the combustion became more complete and the pores gradually developed from semi-closed pores to open pores. At the end of combustion, the pores framework structure gradually weakened, the amount of micropores decreased, and mesopores and macropores gradually collapsed.

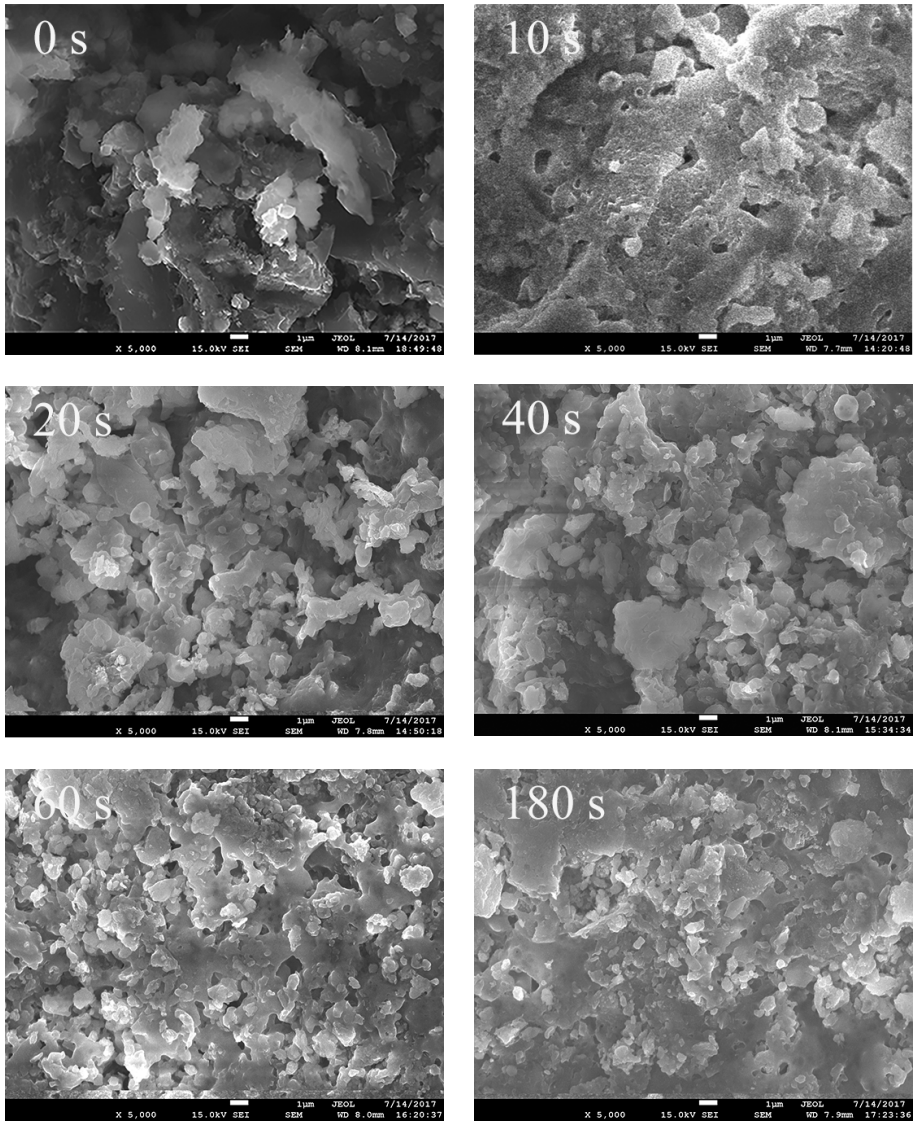

Fig. 7. SEM images of the semicoke sample at different residence times.

3.5. Fractal analysis of semicoke at different residence times

At the beginning of combustion, the precipitation of organic matter led to changes in the Longkou semicoke surface pore structure, and the fractal dimension was constantly rising. As the reaction progressed, thermal stress caused irreversible changes in the pore structure, and the fractal dimension gradually decreased. Figure 8 shows that the overall change trend of the fractal dimension obtained by the adsorption test and that of the box dimension obtained by SEM analysis were basically the same, both of which increased first and then slowly decreased. The physical properties of Longkou oil shale semicoke were complex, and there were many factors such as component, metamorphism and pore size distribution that affected the fractal dimension. The study found that these factors could cause structural heterogeneity in the semicoke space. In the initial stage of semicoke combustion, the precipitation of volatile matter, combustion of semicoke and uneven distribution of pore size led to significant changes in the space structure. In a later stage of combustion, hard minerals were formed, the pore size distribution became uniform and the fractal dimension changes nearly levelled off.

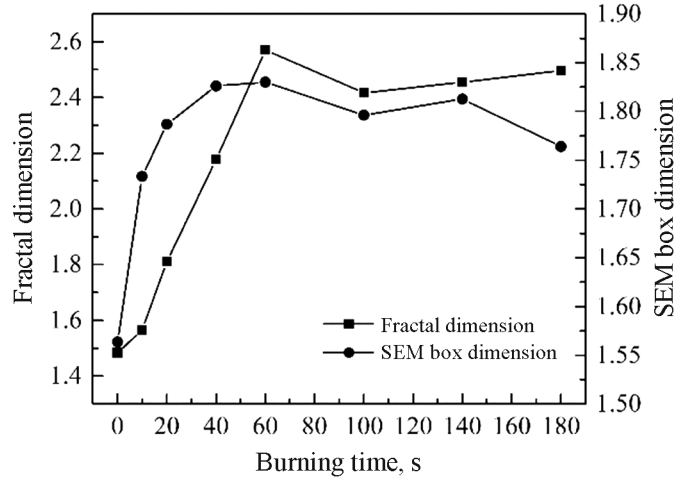

Fig. 8. Variation of the fractal dimension of the semicoke pore structure at different residence times.

4. Conclusions

Based on the experimental study on the combustion of Longkou oil shale semicoke in a batch fluidized bed, it is found that the pore structure of semicoke undergoes a complex process. Also, the reaction time, burning temperature and particle size influence the development of pore structure.

Longkou oil shale semicoke had a developed pore structure, the specific surface area and pore volume increased at first, then decreased, and finally remained stable during combustion, and there were mainly micropores and mesopores of about 2 nm in the structure. As the combustion temperature increased, the pore volume of semicoke first increased and then decreased, and at 400 °C, the specific surface area and pore volume were close to those of the original sample. When the temperature reached 600 °C and 700 °C, the pore structure was fully developed, and the specific surface area and pore volume reached the maximum.When the temperature rose above 700 °C, the excessive temperature caused the destruction of the pore structure, and the specific surface area and pore volume were significantly reduced. The pore size distribution of 3–4 mm semicoke particles was wider than that of 1–2 mm particles, and the pore structure was more complicated.

The microscopic morphology of the sample revealed that the pore structure of the original semicoke sample was developed and the pores assumed different shapes during the combustion process. At 60 s, the amount of micropores began to significantly decrease, and in the pore structure macropores and large cracks started to dominate. The trend of variation of the fractal dimension calculated by the box dimension method and the Frenkel-Halsey-Hill equation was basically the same, and the overall variation trend of the curve was a rapid ascent at first and then a slow descent.

Acknowledgements

This research was supported by the China Scholarship Council (CSC), the National Natural Science Foundation of China (No. 51676032) and the Education Department of Jilin Province (JJKH20190702KJ).

REFERENCES

1. Kok, M. V. Oil shale: pyrolysis, combustion, and environment: A review. *Energ. Source.,* 2002, **24**(2), 135–143.
2. Wang, Q., Bai, J. R., Sun, B. Z., Sun, J. Strategy of Huadian oil shale comprehensive utilization. *Oil Shale*, 2005, **22**(3), 305–316.
3. Pihu, T., Konist, A., Neshumayev, D., Loo, L., Molodtsov, A., Valtsev, A. Full-scale tests on the co-firing of peat and oil shale in an oil shale fired circulating fluidized bed boiler. *Oil Shale*, 2017, **34**(3), 250–262.
4. Maaten, B., Järvik, O., Loo, L., Konist, A., Siirde, A. Characterization of the pyrolytic water from shale oil industry. *Oil Shale*, 2018, **35**(4), 365–374.
5. Konist, A., Loo, L., Valtsev, A., Maaten, B., Siirde, A., Neshumayev, D., Pihu, T. Calculation of the amount of Estonian oil shale products from combustion in regular and oxy-fuel mode in a CFB boiler. *Oil Shale*, 2014, **31**(3), 211–224.

6. Neshumayev, D., Pihu, T., Siirde, A., Järvik, O., Konist, A. Solid heat carrier oil shale retorting technology with integrated CFB technology. *Oil Shale*, 2019, **36**(2S), 99–113.
7. Han, X. X., Kulaots, I., Jiang, X. M., Suuberg, E. M. Review of oil shale semi-coke and its combustion utilization. *Fuel*, 2014, **126**, 143–161.
8. Wang, Q., Zhao, W. Z., Liu, H. P, Jia, C. X., Li, S. H. Interactions and kinetic analysis of oil shale semi-coke with cornstalk during co-combustion. *Appl. Energ.*, 2011, **88**(6), 2080–2087.
9. Trikkel, A., Kuusik, R., Martins, A., Pihu, T., Stencel, J. M. Utilization of Estonian oil shale semicoke. *Fuel Process. Technol.*, 2008, **89**(8), 756–763.
10. Kaljuvee, T., Kuusik, R., Trikkel, A., Radin, M. Behavior of sulphur compounds at combustion of oil shale semicoke. *Oil Shale*, 2003, **20**(2), 113–125.
11. Zanoni, M. A. B., Massard, H., Martins, M. F. Formulating and optimizing a combustion pathway for oil shale and its semi-coke. *Combust. Flame*, 2012, **159**(10), 3224–3234.
12. Liu, H. P., Liang, W. X., Wu, M. H., Wang, Q. Co-combustion of oil shale retorting solid waste with cornstalk particles in a circulating fluidized bed. *Energ. Fuel.*, 2015, **29**(10), 6832–6838.
13. Sun, B. Z., Wang, Q., Tan, P., Liu, H. P., Li, S. H., Guan, X. H. Thermal fragmentation characteristic of oil shale and semi-coke in fluidized bed combustion. *Proceedings of the CSEE*, 2010, **30**(23), 62–66 (in Chinese).
14. Külaots, I., Goldfarb, J. L., Suuberg, E. M. Characterization of Chinese, American and Estonian oil shale semicokes and their sorptive potential. *Fuel*, 2010, **89**(11), 3300–3306.
15. Huang, Y. Q., Zhang, M., Shan, L., Yang, H. R., Yue, G. X. Effects of retorting conditions on pore structure of oil shale semi coke. *CIESC Journal*, 2017, **68**(10), 3870–3876 (in Chinese).
16. Zhao, L. M., Liang, J., Qian, L. X. Study on porous structure and fractal characteristics of oil shale and semicoke. *Adv. Mater. Res.*, 2013, **868**, 276–281.
17. Bai, J. R., Wang, Q., Jiao, G. J. Study on the pore structure of oil shale during low-temperature pyrolysis. *Energy Procedia*, 2012, **17**(Part B), 1689–1696.
18. Qin, H., Sun, B. Z., Wang, Q., Zhou, M. Z., Liu, H. P., Li, S. H. Analysis on influence factors of the characteristic of pore structure during combustion of oil shale semi-coke. *Proceedings of the CSEE*, 2008, **28**(35), 14–20 (in Chinese).
19. Yang, Y. L., Zheng, K. Y., Li, Z. W., Si, L. L., Hou, S. S., Duan, Y. J. Experimental study on pore-fracture evolution law in the thermal damage process of coal. *Int. J. Rock Mech. Min. Sci.*, 2019, **116**, 13–24.
20. Li, H., Shi, S. L., Lu, J. X., Ye, Q., Lu, Y., Zhu, X. N. Pore structure and multifractal analysis of coal subjected to microwave heating. *Powder Technol.*, 2019, **346**, 97–108.
21. Sun, B. Z., Zhou, M. Z., Liu, H. P., Wang, Q., Guan, X. H., Li, S. H. Study on surface characteristics of oil shale during fluidized combustion. *Journal of Power Engineering*, 2008, **28**(2), 250–254 (in Chinese).

22. Rouquerol, J., Avnir, D., Fairbridge, C. W., Everett, D. H., Haynes, J. M., Pernicone, N., Ramsay, J. D. F., Sing, K. S. W., Unger, K. K. Recommendations for the characterization of porous solids. *Pure Appl. Chem.*, 1994, **66**(8), 1739–1758.

Presented by A. Konist
Received April 4, 2019